

# Fabrication of poly(orthanilic acid)–multiwalled carbon nanotubes composite film-modified glassy carbon electrode and its use for the simultaneous determination of uric acid and dopamine in the presence of ascorbic acid

Lei Zhang · Zhige Shi · Qiuhua Lang

Received: 19 March 2010 / Revised: 19 July 2010 / Accepted: 25 July 2010 / Published online: 5 August 2010  
© Springer-Verlag 2010

**Abstract** A multiwalled carbon nanotubes (MWNT) modified glassy carbon electrode (GCE) coated with poly(orthanilic acid) (PABS) film (PABS–MWNT/GCE) has been fabricated and used for simultaneous determination of dopamine (DA) and uric acid (UA) in the presence of ascorbic acid (AA) by differential pulse voltammetry (DPV). Scanning electron microscopy, Fourier transform infrared spectra, and electrochemical techniques have been used to characterize the surface morphology of the PABS–MWNT composite film and the polymerization of ABS on electrode surface. In comparison with the bare GCE and the MWNT-modified GCE, the PABS–MWNT composite film-modified GCE, which combines the advantages of MWNT and the self-doped PABS, exhibits good selectivity and sensitivity for the simultaneous and selective determination of UA and DA in the presence of AA. Due to the different electrochemical responses of AA, DA, and UA, PABS–MWNT/GCE can resolve the overlapped oxidation peak of DA and UA into two well-defined voltammetric peaks with enhanced current responses using both cyclic voltammetry (CV) and DPV. The peak potential separations between DA and UA are 170 mV using CV and 160 mV using DPV, respectively, which are large enough for the selective and simultaneous determination of these species. In the presence of 0.5 mM AA, the DPV peak currents are linearly dependent on the concentration of UA and DA in the range of 6–55 and 9–48  $\mu\text{M}$  with correlation coefficients of 0.997 and 0.993, respectively. The detection limits ( $S/N=3$ ) for detecting UA

and DA are 0.44 and 0.21  $\mu\text{M}$ , respectively. The PABS–MWNT/GCE shows good reproducibility and stability and has been used for the simultaneous determination of DA and UA in the presence of AA in samples with satisfactory results.

**Keywords** Multiwalled carbon nanotubes · Orthanilic acid · Dopamine · Uric acid · Ascorbic acid

## Introduction

It is known that polyaniline (PAN) shows electro-activity only when the medium pH is less than 4; this greatly limits its potential application in practice, especially in bioelectrochemistry, which normally requires a neutral pH environment. To develop the extensive application of PAN, many efforts have been focused on the adaptation of PAN to a higher solution pH. In 1990, Yue and Epstein introduced sulfonic acid group into the PAN backbone to obtain the self-doped PAN for the first time, which can still exhibit its electro-activity in neutral pH medium [1]. Afterwards, many researchers tried to prepare sulfonated PAN including copolymerization of aniline with sulfonated aniline or homopolymerization of ring sulfonated aniline by substituting with electron donating groups or by putting a spacer between the sulfonated group and the ring [2–4]. Many aniline derivatives, especially functionalized with carboxylic acid and sulfonic acid groups, have been widely used in bioelectrochemistry fields due to their good electro-activity over a wide range of pH values [5, 6].

Dopamine (DA) is a neurotransmitter in mammalian central nervous system, which is widely distributed in brain tissues for message transfer and has the cognitive functions of attention, stress, rewarding behavior, and reinforcing effects

L. Zhang (✉) · Z. Shi · Q. Lang  
Department of Chemistry,  
College of Life and Environment Sciences,  
Shanghai Normal University,  
Shanghai 200234, People's Republic of China  
e-mail: chemzl@shnu.edu.cn

of certain stimuli. Low level of DA may cause neurological disorder, such as schizophrenia and Parkinson's disease [7]. Therefore, it is of clinical significance to develop simple and effective methods for measuring DA to prevent these diseases. Among the various methods for detecting DA, electrochemical determination of DA has demonstrated to be a preferred method due to its simplicity, fast response, and high sensitivity. However, the co-existence of ascorbic acid (AA) and uric acid (UA) in biological samples makes it difficult for the selective detection of DA. It is known that the direct redox reactions of these species at bare electrodes are irreversible and therefore require high overpotentials [8], and these compounds have nearly the same oxidation potentials at common electrodes and often suffer from a pronounced fouling effect, which results in rather poor selectivity and reproducibility [9]. Furthermore, since the concentration of DA (<100 nM) is much smaller than that of AA (100–500  $\mu\text{M}$ ) in biological samples [10], both sensitivity and selectivity are of equal importance in developing voltammetric procedures. Up to now, many studies have been reported for selective determination of DA in the presence of AA and/or UA by using various coating films, such as Nafion [11], clay [12], overoxidized polypyrrole [13, 14], polythiophene [15], gold nanoparticles [16], boron-doped diamond [17], multiwalled carbon nanotubes [18, 19], ruthenium oxide [20], titanate nanotube [21], Pt nanoclusters and DNA [22], polypyrrole-1-propionic acid [23], ribonucleic acid [24], fullerene- $\text{C}_{60}$  [25], silica gel [26], carbon nanotubes–ionic liquid gel [27], 2,2-bis(3-amino-4-hydroxyphenyl) hexafluoropropane [28], and so on.

UA is the primary product of urine metabolism, and its inconsistency in human body can induce many diseases, such as gout, hyperuricemia, and Lesch–Nyan diseases [29]. Thus, measuring the amount of UA in biological fluids is of paramount importance in the diagnosis of these diseases. However, the co-existence of AA and UA in body fluids, the high oxidation overpotentials of UA and AA, and the nearly similar oxidation potentials of UA and AA make it difficult for the selective determination of UA at common electrodes [30]. Thus, in the past decades, the selective and simultaneous detection of UA and AA have long been concerned, and various chemically modified electrodes have been fabricated and used for the selective determination of UA in the presence of AA [31, 32], the simultaneous determination of AA and UA [33, 34], and even the simultaneous measurement of AA, DA, and UA [35–38]. Although several works have studied the simultaneous detection of DA and UA [39, 40], considering the co-existence of UA, DA as well as the excess of AA in biological fluids, further efforts should be made to develop simple, selective, and sensitive methods for the simultaneous determination of DA and UA via separating the

oxidation peaks of AA, DA, and UA from one another at electrodes or eliminating the interference of AA.

Considering the high catalytic activity of MWNTs and the good electrochemical activity of the self-doped PABS in a wide pH range and also as a binder for the stable and homogeneous distribution of MWNTs on electrode surface, this work reports the fabrication of the PABS–MWNT composite film-modified GCE by firstly casting well-distributed MWNT suspension on GCE surface (MWNT/GCE) and then performing electrochemical polymerization of orthanilic acid (ABS) at MWNT/GCE. Based on the different electrochemical behaviors of AA, DA, and UA at the PABS–MWNT composite film-modified GCE, the simultaneous determination of DA and UA in the presence of AA at PABS–MWNT/GCE has been studied.

## Experimental

### Chemicals and solutions

All chemicals were commercially available and used as received. The MWNT (98%, produced by current arc-discharge method) was purchased from Shenzhen Nanotech Ltd. Co. (China). ABS and *N*-methyl-pyrrolidone (NMP) were obtained from Fluka. UA, AA, and DA were purchased from Sigma. AA, UA, and DA solutions were prepared with 0.1 M phosphate buffer solutions (PBS, pH 4.5) immediately prior to use. Millipore-filtered water with resistivity of 18.2  $\text{M}\Omega$  was used for all aqueous solutions and rinsing. All other reagents were of analytical quality.

### Apparatus

All electrochemical experiments were performed on a CHI 660C electrochemical analyzer (USA) in a conventional three-electrode electrochemical cell using PABS–MWNT/GCE, MWNT/GCE, and GCE ( $\varnothing=3$  mm) as working electrodes, a platinum sheet ( $1\times 0.5$   $\text{cm}^2$ ) as auxiliary electrode, and a saturated calomel electrode as reference electrode.

Differential pulse voltammetry (DPV) measurements were performed at the potential interval from  $-0.2$  V to  $0.6$  V using a scan rate of  $10$   $\text{mVs}^{-1}$ , pulse amplitude of  $25$  mV, pulse rate of  $0.5$  s, and pulse width of  $60$  ms. During all the electrochemical experiments, the solutions were thoroughly deoxygenated by bubbling high purity nitrogen, and a nitrogen atmosphere was maintained over the solutions. All experiments were made at room temperature ( $\approx 21$   $^{\circ}\text{C}$ ).

The surface morphologies of the modified electrodes were characterized using an S-4800 field emission scanning

electron microscope (Hitachi, Japan). Fourier transform infrared (FTIR) spectrum was recorded on a KBr disk containing about 1% sample by weight using a Nicolet Avatar 370 DTGS (Nicolet, USA) spectrophotometer.

#### Carboxylation treatment of MWNT and fabrication of modified electrode

The MWNT was first purified prior to use by sonicating in 2 M hydrochloric acid for 2 h, and then the purified MWNT was sonicated in nitric acid solution (30%, v/v) for 4 h to obtain the MWNT functionalized with carboxylic acid functionalities. Following the acid treatment, the MWNT were filtered, washed with deionized water, and dried for about 10 h at room temperature (25 °C). Then 1 mg of the MWNT was dispersed in 1 mL ultrapure water and sonicated for 5 min, resulting in a homogeneous black suspension. Prior to surface modification, the GCE was firstly polished with 0.05  $\mu\text{m}$  alumina slurry and cleaned by ultrasonication in water and ethanol successively and dried in a nitrogen atmosphere. Then, 5  $\mu\text{L}$  of the carboxylic-modified MWNT suspension was dropped directly onto the GCE surface and dried at ambient conditions. The MWNT-modified GCE was then immersed into  $1.0 \times 10^{-3}$  M ABS solution (pH 7.0, PBS) and was treated by cyclic scanning between  $-0.2$  and  $1.2$  V at  $50 \text{ mVs}^{-1}$  for 40 min. After thoroughly rinsing with abundant ethanol and water, the PABS–MWNT/GCE was then obtained.

## Results and discussion

#### Characterization of PABS–MWNT/GCE

**Electro-polymerization of ABS on MWNT/GCE** To investigate the polymerization and electrochemical behavior of ABS on MWNT/GCE, the cyclic voltammograms (CVs) recorded for the polymerization of ABS are shown in Fig. 1. As can be seen, in the first cycle, an irreversible oxidation peak is observed at 0.93 V, which could be assigned to the electro-oxidation of ABS to generate the ABS cation radicals (ABSCRs), and after the first potential scanning, another anodic peak was observed at 0.24 V. This peak may be caused by the subsequent generated ABS dimer, which would grow into the final polymer during electrochemical deposition. On the other hand, one can note that the peak current for the oxidation peak located at 0.24 V increased gradually with the continuous potential scanning, while, for the anodic wave at 0.93 V, the peak current decreased gradually with the continuous potential scanning. This is because that, after formation of ABSCRs, they will react each other and also with the ABS monomers

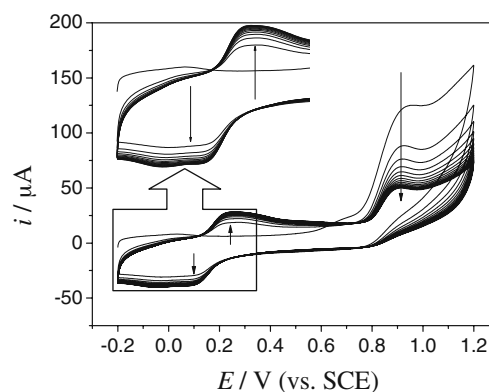


**Fig. 1** CVs of  $1.0 \times 10^{-3}$  M ABS at MWNT/GCE in 0.1 M PBS pH 4.5. Scan rate  $0.05 \text{ Vs}^{-1}$

in solution to generate the ABS dimer; thus, with the continuous generation of ABS dimer, the amount of ABSCRs in solution will decrease gradually, and the amount of ABS dimer will show a corresponding increase. This will, thus, lead to the decrease for the oxidation current of the peak at 0.93 V and the increase for the peak current of the oxidation wave at 0.24 V, and as for the reduction wave at 0.12 V, resulted from the reduction of ABSCRs and ABS dimers, its current response shows gradual increase with the continuous electrolysis. These electrochemical behaviors are the typical characteristics for the polymerization of compound, indicating the deposition of PABS on MWNT/GCE.

To verify the formation of PABS, the obtained polymer film on electrode surface was resolved into NMP for FTIR characterization (Fig. 2). As shown in Fig. 2, the large descending baseline in the spectral region of  $3,500\text{--}2,000 \text{ cm}^{-1}$  is often used to indicate the free-electron conduction in conducting polymers [41]. The broad peak centered at  $3,426 \text{ cm}^{-1}$  is attributed to unresolved N–H stretching mode. Just as that in the PAN structure, the aromatic C–H stretching at  $3,000 \text{ cm}^{-1}$  is weak but detectable. The absorption peaks at 1,594 and  $1,502 \text{ cm}^{-1}$  are due to the

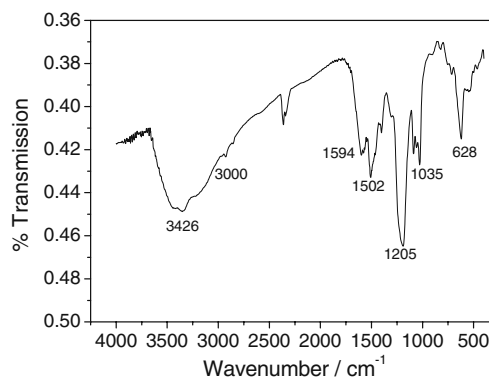


**Fig. 2** FTIR spectrum of PABS

stretching of the benzenoid and quinoid structures. A strong aromatic C–N stretching is responsible for the peak at  $1,205\text{ cm}^{-1}$ . The absorptions at  $1,035$  and  $628\text{ cm}^{-1}$  are the best confirmation for the presence of sulfonate functional groups in the polymer [42]. This indicates the formation of PABS on electrode surface.

To investigate the surface morphology of PABS–MWNT/GCE, the scanning electron microscopy (SEM) image of the obtained modification film is shown in Fig. 3b, and as a comparison, the surface structure of MWNT/GCE is also shown in Fig. 3a. It can be seen from Fig. 3a that the electrode surface is mostly covered with homogeneous MWNTs, and after modification of MWNT/GCE with PABS, the surface image (Fig. 3a) shows clearly that there is a thin and homogeneous PABS film on the surface of MWNTs, indicating the formation of the composite film of PABS–MWNTs.

It should be noted that, in general, CNTs mainly exist in or tend to form the form of big bundles that cannot be totally and efficiently used for electrochemical reaction, while it can be seen from Fig. 3b that the MWNTs confined in the composite film are in the form of small bundles or single tubes. This indicates that the PABS film on the surface of MWNTs cannot only maintain the catalytic activity of MWNTs but also keep the stable and homogeneous distribution of MWNTs on electrode surface. Furthermore, it is believed that the small bundles and

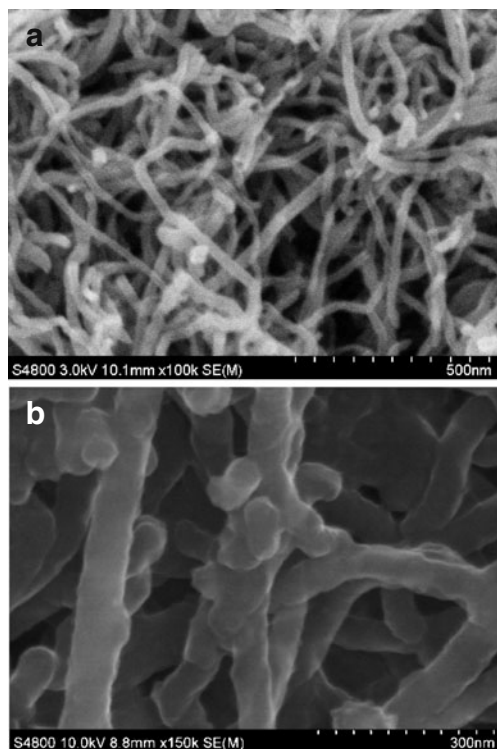


**Fig. 3** SEM images of the surface morphologies of MWNT/GCE (a) and PABS–MWNT/GCE (b)

single tubes are very attractive for electrochemical applications, especially for fabricating electrochemical sensors, because each of the tubes is accessible to many kinds of analytes, and can be used as an electrochemical sensing unit, yielding a sensitive and efficient signal.

#### Redox electro-activity of the PABS–MWNT/GCE

To confirm the improved electrochemical activity of the self-doped PABS coated on MWNT/GCE, the electrochemical behaviors of PABS–MWNT/GCE in solutions with different pH values have been studied (Fig. 4). It can be seen from Fig. 4 that the PABS–MWNT/GCE exhibits good electro-activity over a wide range of pH values up to 9. This is due to the attachment of sulfonic groups onto the PAN backbone, which can change the micro-environment of PAN backbone. It can be assumed that when there is an increase in medium pH, the  $-H^+$  ion in  $-SO_3H$  groups can take a role of a “buffer” and maintain the local pH value to some extent in PAN film near the electrode surface. Thus, the PABS can still exhibit electrochemical activity in solution with higher pH value.

#### Electrochemical behavior of AA, DA, and UA at PABS–MWNT/GCE

*Electro-oxidation of AA, DA, and UA at the PABS–MWNT/GCE* Figure 5 shows the voltammetric responses of AA, DA, and UA at GCE (Fig. 5a), MWNT/GCE (Fig. 5b), and PABS–MWNT/GCE (Fig. 5c), respectively. It can be seen from Fig. 5a that the oxidation waves of AA, DA, and UA at the clean GCE locate at 0.43, 0.45, and 0.52 V, respectively. The current ratio for the oxidation of AA, DA, and UA is 3.8:5.3:6.4. While at the MWNT/GCE (Fig. 5b), the oxidation peak potentials of AA, DA, and UA are observed at 0.13, 0.41, and 0.60 V, respectively. The current ratio for the oxidation of AA, DA, and UA is

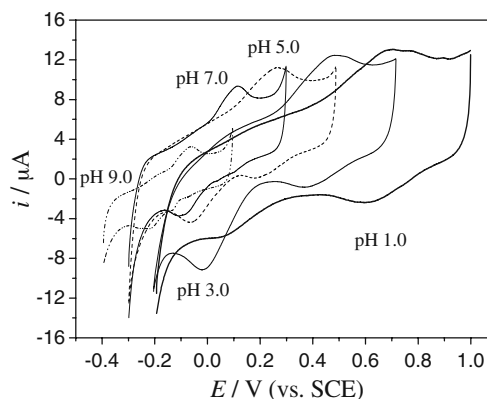


**Fig. 4** CVs of PABS–MWNT/GCE in buffer solutions with different pH values. Scan rate  $0.1\text{ Vs}^{-1}$

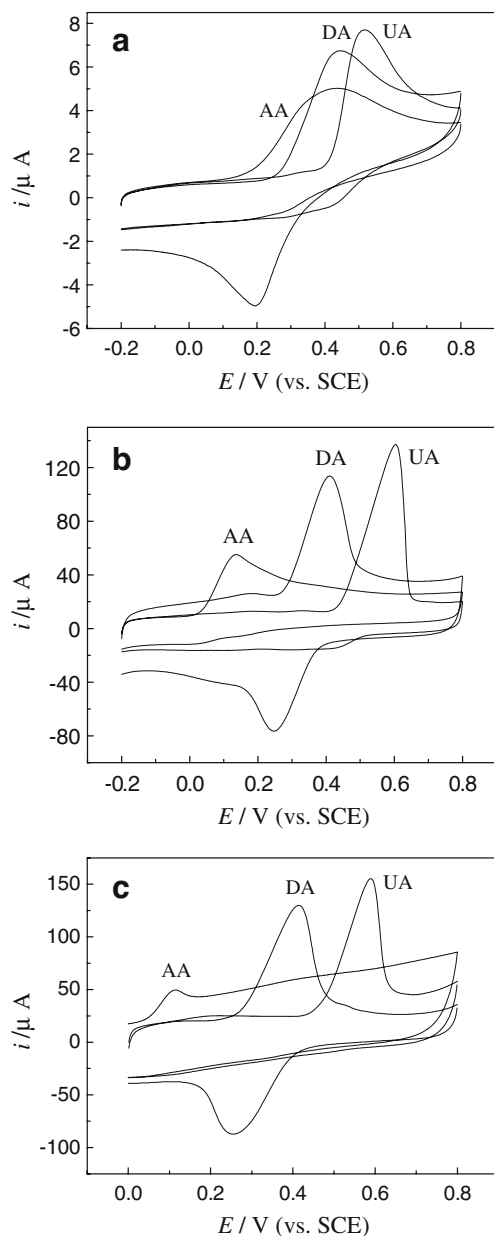


**Fig. 5** CVs of  $1.0 \times 10^{-3}$  M AA,  $1.0 \times 10^{-4}$  M UA, and  $1.0 \times 10^{-4}$  M DA at bare GCE (a), MWNT/GCE (b), and PABS–MWNT/GCE (c) in 0.1 M PBS pH 4.5. Scan rate  $0.1 \text{ V s}^{-1}$

40:86:124. It can be seen from the decreased current ratios for the oxidation of AA, DA, and UA at the MWNT/GCE that the electro-oxidation of AA is suppressed compared with the oxidation of AA at the bare GCE, which is in accordance with the previous report [21]. This could be ascribed to the electrostatic attraction between the negatively charged MWNT and the positively charged UA ( $pK_a=5.75$ ) and DA ( $pK_a=8.87$ ) and the electrostatic expulsion between the negatively charged MWNT film and AA ( $pK_a=4.17$ ). Furthermore, one can see from Fig. 5c that at the PABS–MWNT/GCE, AA, DA, and UA show their oxidation waves at 0.11, 0.41, and 0.58 V,

respectively. The current ratio for the oxidation of AA, DA, and UA is 18:109:135. These results show that the peak current of AA is more decreased compared with that at GCE and MWNT/GCE. The decreased current response for the oxidation of AA and the increased oxidation peak currents for the electro-oxidation of DA and UA at PABS–MWNT/GCE exhibit the electro-catalysis of PABS–MWNT/GCE toward the electro-oxidation of DA and UA. This kinetics effect leads to a substantial increase in the rate of electron transfer between DA and UA and the modified electrode, indicating the improvement in the reversibility of the electron transfer processes [35, 37]. This catalytic function can be attributed to the more favorable interactions between the negatively charged PABS–MWNT composite film and the positively charged DA and UA. The negatively charged PABS–MWNT film can attract the positively charged DA and UA cations to electrode surface and thus enhances their electrochemical responses. At the same time, the rate of electron transfer from AA is decreased as a result of the introduction of the negatively charged modifier (at pH 4.5, the carboxylic acid groups on the surface of the acid-treated MWNT and the sulfonic acid groups bonded on the PAN backbone are deprotonated and negatively charged). The negatively charged PABS–MWNT composite film can repel the negatively charged AA anions from the electrode surface and thus suppresses the electro-oxidation of AA.

*Voltammetric separation for the anodic waves of AA, DA, and UA* Figure 6 shows the voltammetric responses of AA, DA, and UA mixture at bare GCE (Fig. 6a), MWNT/GCE (Fig. 6b, curve a), and PABS–MWNT/GCE (Fig. 6b, curve b), respectively. As shown in Fig. 6a, the bare GCE shows two overlapped voltammetric peak for the oxidation of AA, DA, and UA mixture at about 0.35 V (AA+DA) and 0.51 V (UA), respectively. The voltammetric peaks for the oxidation of AA, DA, and UA are overlapped and indistinguishable; thus, it is impossible to deduce any conclusive information from the overlapped oxidation peaks. While, the MWNT/GCE and PABS–MWNT/GCE can resolve these overlapped oxidation waves into three well-defined voltammetric peaks at 0.08, 0.33, and 0.49 and 0.12, 0.35, and 0.52 V, corresponding to the oxidation of AA, DA, and UA, respectively (curves a and b in Fig. 6b). The current ratios for the electro-oxidation of AA, DA, and UA are 12.5:12:30 and 3.1:12:15, respectively. It can be seen from Fig. 6b (curve b) that the oxidation of AA at PABS–MWNT/GCE is almost completely suppressed. This indicates that the composite film-modified electrode can effectively suppress the electro-oxidation of AA compared with that at MWNT-modified electrode. Thus, the PABS–MWNT/GCE can be used for the selective and simultaneous determination of DA and UA in the presence of AA.

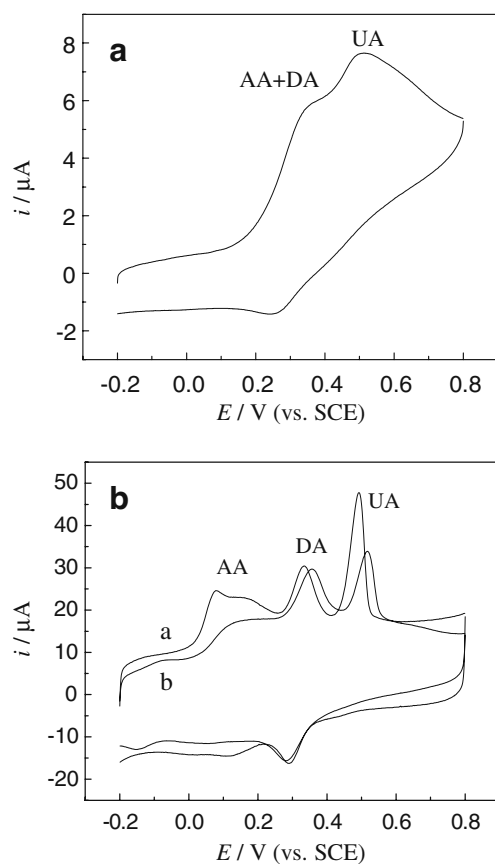


**Fig. 6** CVs of the mixture of  $5.0 \times 10^{-4}$  M AA,  $4.0 \times 10^{-5}$  M UA, and  $9.0 \times 10^{-4}$  M DA at bare GCE (a), MWNT/GCE (curve a in b) and PABS-MWNT/GCE (curve b in b) in 0.1 M PBS pH 4.5. Scan rate  $0.1 \text{ V s}^{-1}$

*Selective determination of UA and DA in the presence of AA* To verify the facility of the PABS-MWNT/GCE for the selective determination of DA in the presence of UA and AA, we investigated the current responses of DA

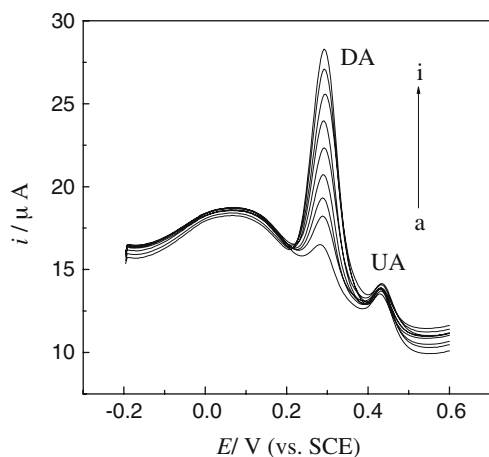


**Fig. 7** DPVs of DA with different concentrations (a–i 4.5, 15, 25, 35, 45, 55, 65, 75, and 85  $\mu\text{M}$ ) at PABS-MWNT/GCE in 0.1 M PBS pH 4.5 in the presence of  $6.0 \times 10^{-6}$  M UA and  $5.0 \times 10^{-4}$  M AA

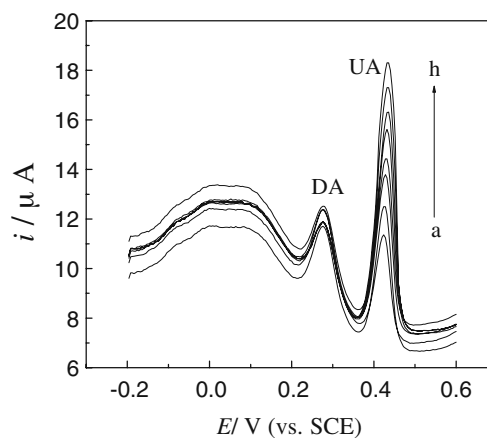


**Fig. 8** DPVs of UA with different concentrations (a–h 10, 20, 30, 40, 50, 60, 70, and 80  $\mu\text{M}$ ) in the presence of  $1.0 \times 10^{-5}$  M DA and  $5.0 \times 10^{-4}$  M AA at PABS-MWNT/GCE in 0.1 M PBS pH 4.5

with different concentrations in the presence of UA and AA (Fig. 7). As shown in Fig. 7, in the presence of UA and AA, the DPV peak current of DA increases linearly with the increasing of DA concentration in the range of 4.5–85  $\mu\text{M}$ , and the current response of UA is nearly stable with the increasing DA contents, while no DPV oxidation peak could be observed for the oxidation of AA. It should be noted that the broad peak centered at about 0.07 V is ascribed to the oxidation of the carboxylic groups on and even inside the MWNT, because when excessive AA is added in solution, this broad wave keeps almost unchanged. These results demonstrate that DA can be detected selectively in the presence of UA and AA by using the PABS-MWNT/GCE. For the regression plot of  $i_p$  vs DA concentration, the slope is  $0.146 \mu\text{A} \mu\text{M}^{-1}$ , the  $y$ -intercept is  $1.03 \mu\text{A}$  and correlation coefficient ( $r^2$ ) is 0.997. The detection limit ( $S/N=3$ ) for DA is  $0.103 \mu\text{M}$ .

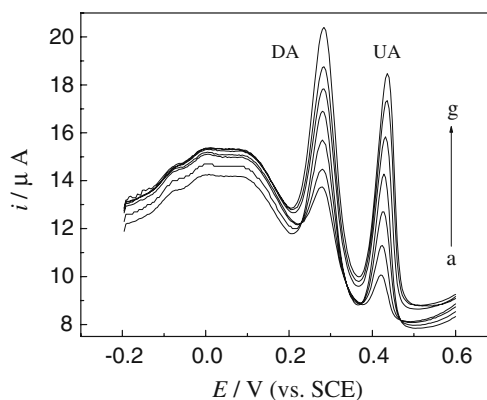


**Fig. 9** DPVs of DA and UA mixtures at PABS-MWNT/GCE in the presence of  $5.0 \times 10^{-4}$  M AA in 0.1 M PBS pH 4.5. DA contents from a to g are 9, 15, 22, 28, 34, 40, and 48  $\mu\text{M}$ . UA contents from a to g are 6, 15, 23, 31, 39, 47, and 55  $\mu\text{M}$

**Table 1** Characteristics of some electrochemical methods for the selective determination of DA and UA in the presence of AA

Working electrode	Method	pH	Peak separation (mV)	Detection limit (μM)		Dynamic range (μM)			Interference of AA	Application	Reference
				DA	UA	DA	DA	UA			
DNA/poly( <i>p</i> -aminobenzenesulfonic acid) bi-layer-modified GCE	DPV	7.0	136	0.088	0.19	0.19–13	0.4–23	1 mM AA does not affect	Not mentioned	[6]	
Prenodized clay-modified GCE	SWV	7.4	–	0.0027	0.2	0–6	0.5–100	Excess AA does not affect	Urine	[12]	
Cu nanoparticles–polypyrrole-modified GCE	DPV	7.0	190	0.003	0.004	0.001–0.1	0.001–10	0.05 mM AA does not affect	DA injection urine	[13]	
Gold nanoparticle–choline-modified GCE	DPV	7.0	140 <sup>a</sup>	0.12	0.6	0.2–80	1.2–100	AA can be neglected	DA injection urine	[14]	
SWCNTs–CPB multilayer films-modified GCE	DPV	7.0	123	0.6	0.7	4–120	2–90	0.4 mM AA does not affect	DA injection	[17]	
Poly(acrylic acid)–MWNT-modified GCE	LSV	7.4	170	0.02	0.11	0.04–3	0.3–10	0.3 mM AA does not affect	Not mentioned	[21]	
DNA–Pt nanocluster-modified GCE	DPV	7.0	140	0.036	0.1	0.11–38	0.3–57	1 mM AA does not affect	Not mentioned	[22]	
RNA-modified GCE	DPV	7.0	144	0.2	0.36	0.37–36	0.74–73	5 mM AA does not affect	Not mentioned	[39]	
Co(TPP), tetraphenyl-borate-modified GCE	LSV	6.5	157 <sup>a</sup>	0.02	0.07	0.06–25	0.1–35	0.1 mM AA does not affect	Urine	[40]	
PABS–MWNT-modified GCE	DPV	4.5	160	0.21	0.44	9–48	6–45	0.5 mM AA does not affect	DA injection	This work	

SWV square wave voltammetry, LSV linear sweep voltammetry, SWCNTs single wall carbon nanotubes, CPB cetylpyridinium bromide, Co(TPP) cobalt(II) tetrakisphenylporphyrin

<sup>a</sup> Studied by CV

It is also known that the electro-oxidation of DA can catalyze the oxidation of UA and AA; thus, the oxidation of UA is influenced by the co-existed DA [43]. Therefore, eliminating this catalytic reaction should be necessary for the accurate determination of UA. However, the results shown in Fig. 7 exhibit that the current response of UA is nearly unchanged with the increasing DA contents in solution. This indicates that the influence resulted from the electro-oxidation of DA on the oxidation of UA has been effectively suppressed at PABS–MWNT/GCE.

To investigate the selective determination of UA in the presence of DA and AA at PABS–MWNT/GCE, the DPV responses of PABS–MWNT/GCE in the mixtures of AA, DA, and UA with different contents have been illustrated in Fig. 8. It can be seen from Fig. 8 that in the presence of DA and AA, the DPV peak currents for the electro-oxidation of UA show linearly relationship with UA concentration in the range of 10–80  $\mu\text{M}$ . For the regression plot of  $i_p$  vs UA concentration, the slope is  $0.26 \mu\text{A} \mu\text{M}^{-1}$ , the  $y$ -intercept is  $7.22 \mu\text{A}$ , and correlation coefficient ( $r^2$ ) is 0.92. The detection limit ( $S/N=3$ ) for DA is  $0.32 \mu\text{M}$ , and also, it can be seen from Fig. 8 that with increasing of UA contents, the current response of DA is nearly stable, which indicates that the homogeneous catalysis of UA and AA can be eliminated at PABS–MWNT/GCE.

**Simultaneous determination of UA and DA in the presence of AA** To further study the application of PABS–MWNT/GCE for the simultaneous analysis of DA and UA in the presence of AA, the DPV responses of their tertiary mixtures by simultaneously changing the concentrations of DA and UA have been investigated (Fig. 9). As can be seen, two well-defined DPV oxidation peaks are obtained at 0.28 and 0.44 V for the electro-oxidation of DA and UA, respectively. The peak separation (0.16 V) between the two oxidation waves is large enough for the simultaneous determination of DA and UA without the influence of AA. The oxidation current of DA increases linearly with its concentration between 9 and 48  $\mu\text{M}$ . For the regression plot of  $i_p$  vs DA concentration, the slope is  $0.18 \mu\text{A} \mu\text{M}^{-1}$ , the  $y$ -intercept is  $8.95 \mu\text{A}$ , and the correlation coefficient ( $r^2$ ) is 0.993. The detection limit ( $S/N=3$ ) for DA detection is

$0.21 \mu\text{M}$ , and for the determination of UA, the calibration plot of UA is linear from 6 to 55  $\mu\text{M}$  with slope, intercept, and correlation coefficient of  $0.21 \mu\text{A} \mu\text{M}^{-1}$ ,  $8.96 \mu\text{A}$ , and 0.997, respectively, and the detection limit ( $S/N=3$ ) is  $0.44 \mu\text{M}$ . This shows that the fabricated modified electrode can be used for the simultaneous determination of DA and UA in the presence of AA. Compared with the studies on the simultaneous determination of DA and UA in the presence of AA, as shown in Table 1, the present procedure shows high selectivity and good sensitivity.

To investigate the practicality of the proposed method, the PABS–MWNT/GCE had been used for the selective detection of DA in dopamine hydrochloride injection (DHI) solution, in which certain amounts of AA and UA had been added previously. To fit the calibration curve and decrease the matrix effect, the DHI (10 mg DA/mL, 2 mL per injection) was firstly diluted ten times with 0.1 M pH 4.5 PBS, then 5 mL of the diluted injection as well as 2 mL UA (0.1 mM), and 1 mL AA (5 mM) standard solutions were added to a series of 10 mL measuring flasks and made up to volume with 0.1 M PBS pH 4.5. After putting an aliquot of 3.0 mL of the sample solution into electrochemical cell, the concentrations of DA and UA were determined by the proposed calibration method. Results are shown in Table 2. The recovery rates are in the ranges of 97.9–101.7% for DA and 98.8–101.3% for UA, respectively. The good agreement with the standard content indicates the practicality of the modified electrode for the simultaneous determination of DA and UA in the presence of AA in samples.

#### Interference study

The influence of some foreign species on the detection of 45  $\mu\text{M}$  DA and 45  $\mu\text{M}$  UA in the presence of 500  $\mu\text{M}$  AA had been investigated. The tolerance limit was taken as the maximum concentration of the foreign substances, which caused an approximately  $\pm 5\%$  relative error in the determination. The tolerated concentration of some foreign substances was 0.12 M for  $\text{Na}^+$ ,  $\text{Cl}^-$ , and  $\text{K}^+$ ; 0.075 M for  $\text{Mg}^{2+}$  and  $\text{Ca}^{2+}$ ; and 0.005 M for L-lysine, glucose, glycine, L-asparagine, and glutamic acid. However, when

**Table 2** Simultaneous determination of DA and UA in the presence of AA

No.	Content ( $\mu\text{M}$ )	Spiked ( $\mu\text{M}$ )		Found ( $\mu\text{M}$ )		Recovery (%)	
		AA	UA	UA	DA	UA	DA
1	26.38	500	20	19.82	26.10	99.1	98.9
2	26.38	500	20	20.14	26.59	100.7	100.8
3	26.38	500	20	19.76	26.82	98.8	101.7
4	26.38	500	20	20.23	25.83	101.2	97.9
5	26.38	500	20	20.25	25.88	101.3	98.1



25  $\mu\text{M}$  NADH or 50  $\mu\text{M}$  epinephrine was co-existed in the solution, the relative error of more than  $\pm 5\%$  would be obtained. This is because that the modified GCE also shows good electro-activity toward the electro-oxidation of these species. The details about the electrochemical oxidation of NADH and epinephrine at the modified electrode are under investigation.

#### Electrode reproducibility and stability

To study the reproducibility of the modified electrode, repetitive measurements had been carried out for simultaneous detection of 35  $\mu\text{M}$  UA and 45  $\mu\text{M}$  DA in the presence of 0.50 mM AA. The results of 15 successive measurements showed a relative standard deviation of 3.4% for DA and 5.3% for UA, respectively, indicating that the modified electrode has a good reproducibility and does not undergo surface fouling. After measurements, the modified electrode was cleaned via potential cycling in the range of  $-0.4$ – $1.0$  V ( $0.1$   $\text{Vs}^{-1}$ ) in 0.1 M PBS pH 4.5 to eliminate the absorption till a stable background was obtained, then the electrode was stored in 0.1 M PBS pH 4.5 at room temperature, and the current response was decreased about 5.2% in 1 week and 11% in 2 weeks, indicating the stability of this modified electrode is satisfactory.

#### Conclusions

This study reports the fabrication of the PABS–MWNT composite film-modified GCE and its use for the simultaneous determination of DA and UA in the presence of AA. Due to the formation of self-doped PABS via attachment of sulfonic acid groups onto the backbone of PAN, the PABS exhibits good electro-activity in solutions with a wide range of pH values. Based on the electrostatic attraction between the negatively charged PABS–MWNT composite film and the positively charged DA and UA, the electrochemical responses of DA and UA have been greatly enhanced. In contrast, the electro-oxidation of AA has been greatly suppressed due to the electrostatic repulsion between the negatively charged PABS–MWNT/GCE and the same charged AA. Thus, the PABS–MWNT/GCE can be used for the selective and simultaneous determination of DA and UA in the presence of AA based on the different electrochemical responses of DA, UA, and AA. The proposed method has been successfully applied for detecting DA and the added UA in DHI sample in the presence of AA.

**Acknowledgments** This work was supported by the Innovation Program of Shanghai Municipal Education Commission (09YZ161) and the Natural Science Foundation of Shanghai (09ZR1423500).

#### References

1. Yue J, Epstein AJ (1990) *J Am Chem Soc* 112:2800–2801
2. Mav I, Zigon M, Sebenik A (1999) *Synth Met* 101:717–718
3. Mu S, Kan J (2002) *Synth Met* 132:29–33
4. Zhang L (2007) *J Solid State Electrochem* 11:365–371
5. Zhang L, Zhang CH, Lian JY (2008) *Biosens Bioelectron* 24:690–695
6. Lin XQ, Kang GF, Lu LP (2007) *Bioelectrochemistry* 70:235–244
7. Ali SR, Ma Y, Parajuli RR, Balogun Y, Lai WYC, He H (2007) *Anal Chem* 79:2583–2587
8. Adams RN (1976) *Anal Chem* 48:1126A–1138A
9. Parsons LH, Justice JB Jr (1992) *J Neurochem* 58:212–218
10. O'Neill RD (1994) *Analyst* 119:767–779
11. Lacroix M, Bianco P, Lojou E (1999) *Electroanalysis* 11:1068–1076
12. Zen JM, Chen PJ (1997) *Anal Chem* 69:5087–5093
13. Zhang XJ, Ogorevc B, Tavcar G, Svegl IG (1996) *Analyst* 121:1817–1822
14. Pihel K, Walker QD, Wightman RM (1996) *Anal Chem* 68:2084–2089
15. Gao Z, Yap D, Zhang Y (1998) *Anal Sci* 14:1059–1063
16. Goyal RN, Aliumar A, Oyama M (2009) *J Electroanal Chem* 631:58–61
17. Poh WC, Loh KP, Zhang WD, Sudhiranjan T, Ye JS, Sheu FS (2004) *Langmuir* 20:5484–5492
18. Shahrokhian S, Zare-Mehrjardi HR (2007) *Electrochim Acta* 52:6310–6317
19. Chen PY, Vittal R, Nien PC, Ho KC (2009) *Biosens Bioelectron* 24:3504–3509
20. Shakkthivel P, Chen SM (2007) *Biosens Bioelectron* 22:1680–1687
21. Liu AH, Wei MD, Honma I, Zhou HS (2006) *Adv Funct Mater* 16:371–376
22. Zheng Y, Lin XQ (2008) *Chin J Chem* 26:898–904
23. Milczarek G, Ciszewski A (2004) *Electroanalysis* 16:1977–1983
24. Kang GF, Lin XQ (2006) *Electroanalysis* 18:2458–2466
25. Goyal RN, Gupta VK, Bachheti N, Sharma RA (2008) *Electroanalysis* 20:757–764
26. Nasri Z, Shams E (2009) *Electrochim Acta* 54:7416–7421
27. Zhao YF, Gao YQ, Zhan DP, Liu H, Zhao Q, Kou Y, Shao YH, Li MX, Zhuang QK, Zhu ZW (2005) *Talanta* 66:51–57
28. Zhou L, Shang FJ, Pravda M, Glennon JD, Luong JHT (2009) *Electroanalysis* 21:797–803
29. Wu SG, Wang TL, Gao ZY, Xu HH, Zhou BN, Wang CQ (2008) *Biosens Bioelectron* 23:1776–1780
30. Liu AH, Honma I, Zhou HS (2007) *Biosens Bioelectron* 23:74–80
31. Fang B, Jiao SF, Li MG, Tao HS (2006) *Anal Bioanal Chem* 386:2117–2122
32. Ndamanisha JC, Guo LP (2008) *Biosens Bioelectron* 23:1680–1685
33. Kannan P, Abraham JS (2009) *Anal Biochem* 386:65–72
34. Babaei A, Zendejdel M, Khalilzadeh BL, Taheri A (2008) *Colloids Surf B* 66:226–232
35. Liu Y, Huang JS, Hou HQ, You TY (2008) *Electrochem Commun* 10:1431–1434
36. Zhang R, Jin GD, Chen D, Hu XY (2009) *Sens Actuators B* 138:174–181
37. Zhu SY, Li HJ, Niu WX, Xu G (2009) *Biosens Bioelectron* 25:940–943
38. Yogeswaran U, Chen SM (2007) *Electrochim Acta* 52:5985–5996
39. Kang GF, Lin XQ (2006) *Electroanalysis* 18:2458–2466
40. Zeng YL, Li CX, Tang CR, Zhang XB, Shen GL, Yu RQ (2006) *Electroanalysis* 18:440–448
41. Cao Y, Li S, Xue Z, Guo D (1986) *Synth Met* 16:305–315
42. Conley R (1972) *Infrared spectroscopy*, 2nd edn. Allyn and Bacon, Boston, pp 196–198
43. Alwarappan S, Liu GD, Li CZ (2010) *Nanomedicine* 6:52–57